

Site-Specific Mapping and Time-Resolved Monitoring of Lysine Methylation by High-Resolution NMR Spectroscopy

François-Xavier Theillet, Stamatios Liokatis, Jan Oliver Jost,[†] Beata Bekei, Honor May Rose, Andres Binolfi, Dirk Schwarzer,[†] and Philipp Selenko*

Leibniz Institute of Molecular Pharmacology (FMP Berlin), Robert Roessle Strasse 10, 13125 Berlin, Germany

S Supporting Information

ABSTRACT: Methylation and acetylation of protein lysine residues constitute abundant post-translational modifications (PTMs) that regulate a plethora of biological processes. In eukaryotic proteins, lysines are often mono-, di-, or trimethylated, which may signal different biological outcomes. Deconvoluting these different PTM types and PTM states is not easily accomplished with existing analytical tools. Here, we demonstrate the unique ability of NMR spectroscopy to discriminate between lysine acetylation and mono-, di-, or trimethylation in a site-specific and quantitative manner. This enables mapping and monitoring of lysine acetylation and methylation reactions in a nondisruptive and continuous fashion. Time-resolved NMR measurements of different methylation events in complex environments including cell extracts contribute to our understanding of how these PTMs are established *in vitro* and *in vivo*.

Protein lysine residues are subject to two main types of chemically distinct post-translational modifications (PTMs): lysine acetylation and lysine methylation. Here, we describe time-resolved, high-resolution NMR experiments to monitor lysine acetylation and methylation reactions in parallel. We identify the key NMR characteristics of lysine mono-, di-, and trimethylation and outline experimental approaches to identify lysine methylation states and to map specific lysine methylation sites in a residue-resolved manner both *in vitro* and in complex environments such as mammalian cell extracts.

While acetylation neutralizes the positive charge of lysine residues (Figure 1a), lysine methylation does not (Figure 1b). In addition, lysines can be mono-, di-, or trimethylated. These differences in chemical and physical properties of lysine side chains have important functional consequences, especially in acting as switches to signal different biological responses.^{1–4} In many instances, a given lysine residue can exist in either an acetylated or a differentially methylated form. Variations in lysine acetylation/methylation are therefore tightly controlled and of fundamental importance in many areas of eukaryotic biology.

In contrast to other analytical methods,^{5–7} high-resolution NMR spectroscopy can detect differentially modified lysine residues in a straightforward manner. As acetylated and methylated lysines display very different NMR properties, it is easy to discriminate between these two PTMs. We and others have previously delineated the NMR characteristics of lysine

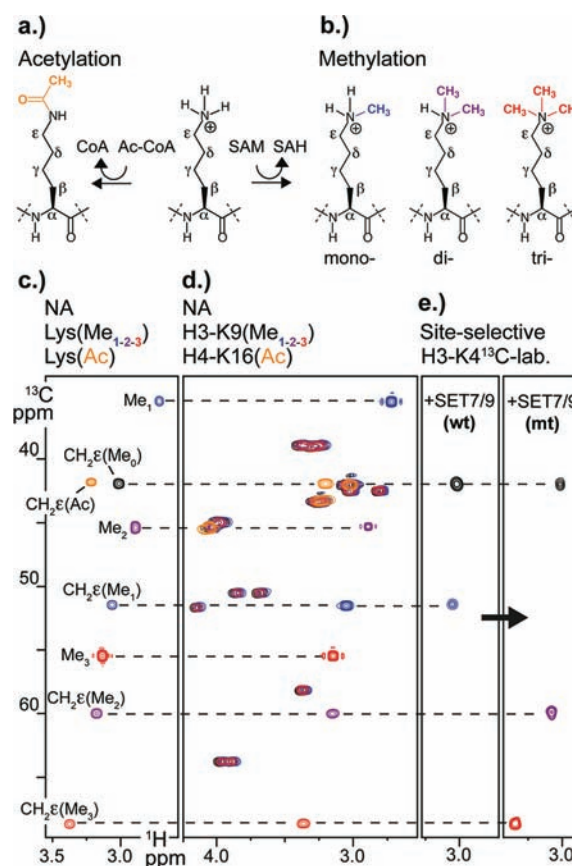


Figure 1. Chemical structures of (a) acetylated and (b) mono-, di-, and trimethylated lysines. (c) Overlay of 2D natural abundance (NA) ¹H–¹³C correlation spectra of non-, mono-, di-, and trimethylated and acetylated lysines (black, blue, purple, red, and orange, respectively). (d) Overlay of 2D NA ¹H–¹³C correlation spectra of histone H3 (aa1–20) non-, mono-, di-, and trimethylated on K9, and of histone H4 (aa1–19) acetylated on K16. (e) Overlay of 2D ¹H–¹³C correlation spectra of H3 (aa1–15), site-selective K4 ¹³C-labeled, monomethylated by wild-type (wt) SET7/9, and successively di- and trimethylated by mutant (mt) SET7/9 (Y245A).

acetylation.^{8–10} In brief, acetylation results in upfield chemical shift changes ($\Delta\delta(^1\text{H}) \approx 0.1$ ppm) of backbone amide resonances of the modified lysine residues that are readily detected in 2D heteronuclear (¹H–¹⁵N) correlation experiments.

Received: February 26, 2012

Published: April 23, 2012

In addition, each acetylation event produces one additional amide resonance signal, the generic *acetylation indicator* at $\sim 7.9/127.5$ ppm (^1H - ^{15}N) that corresponds to the newly formed side-chain amide group of the modified lysine residue (Figure 1a).

Lysine mono-, di-, or trimethylation does not lead to detectable lysine backbone amide chemical shift changes (data not shown). Instead, methylation produces characteristic changes in proton/carbon (^1H - ^{13}C) lysine side-chain correlations (Figure 1c). Especially lysine $\text{CH}_2\epsilon$ resonances experience large ^{13}C downfield chemical shift changes upon methylation. $\text{CH}_2\epsilon$ groups of non-methylated lysines ($\text{CH}_2\epsilon\text{-Me}_0$) resonate at $\sim 3.0/42.0$ ppm (^1H - ^{13}C), while mono- ($\sim 3.1/51.0$ ppm, $\text{CH}_2\epsilon\text{-Me}_1$), di- ($\sim 3.2/60.0$ ppm, $\text{CH}_2\epsilon\text{-Me}_2$), or trimethylated ($\sim 3.4/68.5$ ppm, $\text{CH}_2\epsilon\text{-Me}_3$) lysines display uniquely different correlation signals. In contrast, $\text{CH}_2\epsilon$ resonances of acetylated lysines display characteristic downfield chemical shift changes in the proton dimension ($\sim 3.15/42.0$ ppm, $\text{CH}_2\epsilon\text{-Ac}$), which enables facile discrimination between non-modified, acetylated, or methylated lysines (Figure 1c). Lysine methyl groups resonate at $\sim 2.7/35.5$ ppm (mono-, Me_1), $\sim 2.9/45.5$ ppm (di-, Me_2), or $\sim 3.1/55.5$ ppm (trimethyl, Me_3), while the methyl groups of acetyl-lysines have a resonance frequency of $\sim 2.0/24.0$ ppm (acetyl, Ac), as also reported previously.^{11–13} Because most modifiable lysine residues in folded and unfolded proteins are solvent exposed and sample similar chemical environments, the aforementioned NMR properties are generally preserved (Figure 1d and unpublished data). Thus, lysine $\text{CH}_2\epsilon$ resonances function as unique identifiers of acetylation and methylation states and additionally report the respective forms of lysine methylation in an unbiased manner.

We set out to explore the suitability of these NMR properties to report lysine methylation states by probing a prototypic lysine methyltransferase (KMT), recombinant SET7/9, on histone H3. In a reaction with a synthetic H3 peptide (aa1–15), selectively ^{13}C -labeled at Lys4 (K4), wild-type (wt) SET7/9 displayed exclusive monomethylation (Figure 1e), in line with published data.¹⁴ A SET7/9 mutant (mt, Y245A) further di- and trimethylated K4 when the substrate was presented in a pre-monomethylated form (Figure 1e).^{14,16} Together, these results indicated that NMR monitoring of H3 K4 methylation correctly reported the known modification behaviors of wt and mt SET7/9.

We set up a tailored ^1H - ^{13}C presat-SOFAST-HMQC pulse sequence¹⁵ to specifically detect lysine $\text{CH}_2\epsilon$ resonances with high sensitivity (Figure S1, Supporting Information), which, in turn, enables rapid quantifications of lysine methylation states by simple cross-peak integration routines. Following this rationale, methylated lysine residues in substrates at concentrations as low as $12.5 \mu\text{M}$ (^{13}C -labeled) are accurately quantified within 30 min of experimental time (experimental error $\pm 2\%$). The same level of precision is achieved 4 times faster at twice this concentration and with the same number of scans, as the NMR signal-to-noise ratio increases linearly with concentration, or with the square of the number of scans. Hence, kinetics of enzymatic methylation reactions that produce at least $5 \text{ pmol}\cdot\text{min}^{-1}$ of methylated substrate species can be reported reliably.

To exemplify this notion, we followed the methylation kinetics of SET7/9 by time-resolved NMR monitoring using the above pulse scheme. Initial velocity measurements of methylation rates at different substrate concentrations ($12.5 \mu\text{M}$

to 1.2 mM) were performed with an average quantification error of $\pm 0.25 \mu\text{M}$, or 75 pmol (Figure 2a). Linear fitting to the

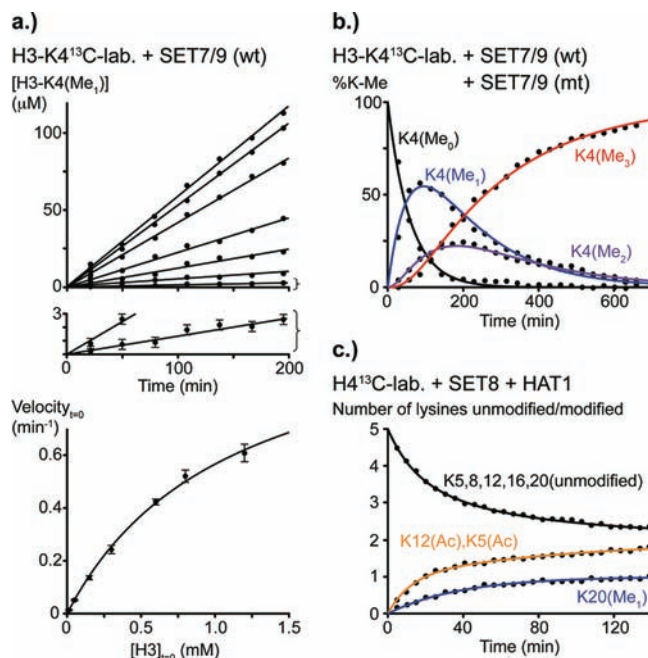


Figure 2. (a) Top: Histone H3 K4 monomethylation kinetics by SET7/9 (wt). The expansion below depicts the sizes of measurement errors due to experimental noise at the lowest enzyme concentration. Bottom: Michaelis–Menten plot of initial velocities against H3 substrate concentrations. Error bars were obtained from two independent measurements. (b) Build-up curves of simultaneous H3 ($100 \mu\text{M}$) K4 mono-, di-, and trimethylation in a mixture of wt and mt SET7/9. (c) Build-up curves of simultaneous H4 ($100 \mu\text{M}$) K20 monomethylation by SET8 and H4 K12 and K5 acetylation by HAT1. Conversion percentages are calculated from NMR signal integrals (Figure S2, Supporting Information). For clarity, only NMR time points at (b) 30 or (c) 5 min intervals are shown.

Michaelis–Menten kinetic model revealed a $k_{\text{cat}} = 1.1 \pm 0.1 \text{ min}^{-1}$ and $K_{\text{m}} = 1.1 \pm 0.2 \text{ mM}$. These values are in excellent agreement with previously reported methylation rates that had been obtained in spectrophotometric assays.¹⁴ We also delineated the respective modification characteristics in a mixed (wt and mt SET7/9) reaction setup (Figure 2b). As expected, H3 K4 monomethylation preceded di- and trimethylation, indicating that mechanistic insights into the SET7/9-specific methylation behavior could unambiguously be obtained from a single set of time-resolved NMR experiments.

As lysine acetylation and methylation produce distinctively different ^1H - ^{13}C correlations, we asked whether we could monitor and individually characterize both types of PTMs in the same NMR experiment. To answer this question, we set up a mixed acetylation/methylation reaction using uniformly ^{13}C -labeled histone H4 (aa1–26) and catalytic amounts of unlabeled, recombinant HAT1 and SET8 (Figures 2c and S2). We had previously shown that the acetyltransferase HAT1 exclusively modified K5 and K12 of histone H4.⁹ SET8, in turn, is a well-characterized H4 K20-specific monomethyltransferase.¹⁷ Following the respective modification profiles by time-resolved 2D ^1H - ^{13}C correlation experiments, we found that both PTM reactions produced NMR readouts that quantitatively reported the individual modification events. Moreover, both kinetic profiles suggested that acetylation of H4 K5 and K12,

and methylation of K20, did not influence each other and proceeded with similar rates as under isolated conditions (data not shown).

While NMR monitoring of lysine methylation based on the aforementioned NMR chemical shift parameters is straightforward, site-specific mapping of individual methylation sites is more challenging. Due to the limited chemical shift dispersion of lysine side-chain resonances (^1H - ^{13}C) in peptides and proteins, all residue-specific information about methylation sites provided thus far was solely afforded by site-selective ^{13}C -lysine labeling or existing knowledge about KMT target sites. To also enable *de novo* NMR mapping of methylated lysine residues, we took advantage of the large $\text{C}\epsilon$ -carbon chemical shift differences between non-, mono-, di-, and trimethylated lysines and the superior chemical shift dispersion of lysine backbone amide resonances in 2D ^1H - ^{15}N correlation spectra. A 2D ($\text{HC}\epsilon$ - (Me_x) -TOCSY- $\text{C}\alpha$)NH pulse scheme was developed in which lysine $\text{CH}_2\epsilon$ resonances were selectively excited at either the mono-, di-, or trimethylated resonance frequency (Figure S3). In combination with lysine-selective $^{15}\text{N}/^{13}\text{C}$ labeling schemes, only those lysine residues that exist in matched methylation states give rise to 2D ^1H - ^{15}N correlation cross-peaks.

Therefore, "scanning" of the characteristic $\text{CH}_2\epsilon$ - Me_x resonance frequencies enables residue-specific mapping of correspondingly methylated lysine residues. To exemplify this notion, we reacted lysine-specific $^{15}\text{N}/^{13}\text{C}$ -labeled histone H2A (aa1–23) with wt SET7/9 (Figure 3a). Multisite methylation of N-terminal histone H2A by wt SET7/9 has recently been reported, but the respective methylation sites had not been identified.¹⁸ NMR measurements revealed that SET7/9 monomethylated H2A K5, K13, and K15, but not K9 (Figure 3b). No di- or trimethylated species were detected (data not shown). 2D ($\text{HC}\epsilon$ - (Me_x) -TOCSY- $\text{C}\alpha$)NH NMR spectra were acquired on 50 μM H2A samples (15 nmol) within 4 h of acquisition time. Hence, the outlined scheme proved particularly suitable to map methylation sites, as well as to identify the respective methylation states. Alternatively, fast 2D ^1H - ^{13}C experiments can initially be employed to qualitatively check for the presence of methylated lysine residues, to monitor the progression of lysine methylation in a time-resolved fashion, and to identify the types of methylation states that are being established. The TOCSY-type NMR experiment may then be used to map the respective methylation sites.

To determine whether it was possible to directly monitor lysine methylation reactions by endogenous KMTs in cellular environments, we prepared whole-cell lysates from cultured human HeLa cells, to which we added recombinant $^{15}\text{N}/^{13}\text{C}$ -lysine-labeled histone H3 (aa1–33), C-terminally protected by fusion to the *Streptococcal* protein G B1 domain (GB1). The GB1 moiety prevented unspecific C-terminal proteolysis of the histone H3 peptide, which was observed at prolonged extract incubation times (>6 h). By time-resolved NMR spectroscopy, we detected lysine mono- and subsequent dimethylation in a highly reproducible manner in different extract preparations (Figure 3b). Minor trimethylation ($\sim 1\%$) was only observed at later time points (data not shown). The initial rate of monomethylation for 200 μM substrate was determined to correspond to $50 \pm 10 \text{ pmol}\cdot\text{min}^{-1}$ per milligram of total lysate proteins. Employing the ($\text{HC}\epsilon$ - (Me_2) -TOCSY- $\text{C}\alpha$)NH NMR experiment, dimethylation was mapped to H3 K9 and/or K27 (Figure 3b). Due to spectral overlap, no unambiguous assignment of the methylation site(s) could be obtained. However, both residues have been identified as mono- and

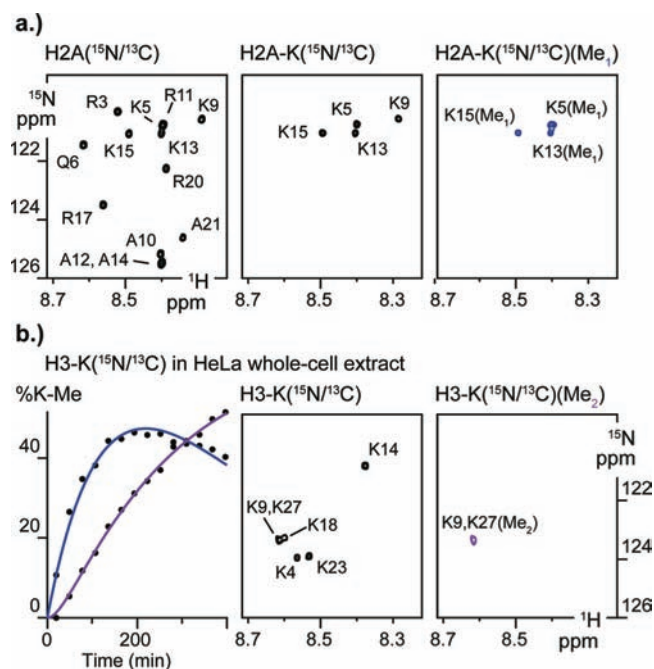


Figure 3. (a) Left: Selected region of the 2D ^1H - ^{15}N correlation spectrum of uniformly labeled histone H2A (aa1–23, 150 μM). Middle: Same region of the 2D ^1H - ^{15}N correlation spectrum of $^{15}\text{N}/^{13}\text{C}$ lysine-selective labeled H2A. Right: Identical view of the 2D ($\text{HC}\epsilon$ - (Me_1) -TOCSY- $\text{C}\alpha$) ^1H - ^{15}N NMR spectrum, showing monomethylated H2A lysines K5, K13, and K15, but not K9, after the reaction with SET7/9. (b) Left: Time course of lysine mono- and dimethylation of H3 (aa1–33)-GB1 (200 μM) in HeLa cell extracts. Middle: Selected region of the 2D ^1H - ^{15}N correlation spectrum of lysine-selective labeled H3 (aa1–33)-GB1. Right: Identical view of the 2D ($\text{HC}\epsilon$ - (Me_2) -TOCSY- $\text{C}\alpha$) ^1H - ^{15}N NMR spectrum shows dimethylated H3 lysines K9 and/or K27, after the reaction in HeLa extracts.

dimethylation substrate sites for several cellular KMTs, including G9a and GLP,^{19–21} which establish transcriptionally silent chromatin structures *in vivo*.^{22,23} Both KMTs also methylate the transcription factor and oncoprotein p53²⁴ and constitute prominent drug targets for cancer therapy.²⁵

In summary, NMR monitoring of lysine methylation and acetylation by 2D ^1H - ^{13}C correlation experiments offers a convenient means to confirm the presence and nature of these PTMs and, in the case of lysine methylation, to determine the respective methylation states. In comparison to other analytical methods,⁵ which are mostly based on indirect readout schemes that require narrowly defined *in vitro* experimental setups and preclude measurements in complex environments such as cell extracts, time-resolved NMR spectroscopy enables direct quantitative monitoring of acetylation and methylation reactions in parallel. While these extract-based NMR measurements may not accurately reflect the spatially controlled enzyme activities of intact cells, they nevertheless enable comparative assessments of global HAT and KMT activities of different cellular environments and of changes in enzymatic activities upon internal or external cues. Methyl- and acetyltransferase enzymes, as well as their demethylating counterparts, i.e., demethylases and deacetylases, constitute prominent drug targets.^{26–29} The unique advantages of NMR spectroscopy for studying these enzymes make it an ideal tool to analyze their modes of action *in vitro* and to elucidate the mechanisms by which they regulate the *writing* and *reading* of PTM-based

signaling codes in complex environments such as cell extracts and possibly also intact cells.

■ ASSOCIATED CONTENT

📄 Supporting Information

Supplementary figures, materials and methods, and NMR pulse sequences. This material is available free of charge via the Internet at <http://pubs.acs.org>.

■ AUTHOR INFORMATION

Corresponding Author

selenko@fmp-berlin.de

Present Address

[†]Interfaculty Institute of Biochemistry (IFIB), University of Tübingen, Hoppe-Seyler-Str. 4, D-72076 Tübingen, Germany

Notes

The authors declare no competing financial interest.

■ ACKNOWLEDGMENTS

We thank Dr. Raymond C. Trievel for providing the expression plasmids for SET7/9 and SET8, Dr. Wolfgang Fischle for control HeLa nuclear extracts, and Dr. Peter Schmieder and Monika Beerbaum for excellent NMR infrastructure maintenance. F.-X.T was supported by a postdoctoral grant from the Association pour la Recherche contre le Cancer (ARC). P.S. is supported by an Emmy Noether program grant (SE-1794/1-1) by the Deutsche Forschungs Gemeinschaft (DFG).

■ REFERENCES

- (1) Barth, T. K.; Imhof, A. *Trends Biochem. Sci.* **2010**, *35*, 618–626.
- (2) Choudhary, C.; Kumar, C.; Gnäd, F.; Nielsen, M. L.; Rehman, M.; Walther, T. C.; Olsen, J. V.; Mann, M. *Science* **2009**, *325*, 834–840.
- (3) Egorova, K. S.; Olenkina, O. M.; Olenina, L. V. *Biochemistry (Moscow)* **2010**, *75*, 535–548.
- (4) Bannister, A. J.; Kouzarides, T. *Cell Res.* **2011**, *21*, 381–395.
- (5) Luo, M. *ACS Chem. Biol.* **2012**, *7*, 443–463.
- (6) Zhang, K.; Yau, P. M.; Chandrasekhar, B.; New, R.; Kondrat, R.; Imai, B. S.; Bradbury, M. E. *Proteomics* **2004**, *4*, 1–10.
- (7) Zee, B. M.; Levin, R. S.; Dimaggio, P. A.; Garcia, B. A. *Epigen. Chromatin* **2010**, *3*, 22.
- (8) Smet-Nocca, C.; Wieruszkeski, J. M.; Melnyk, O.; Benecke, A. *J. Pept. Sci.* **2010**, *16*, 414–423.
- (9) Liokatis, S.; Dose, A.; Schwarzer, D.; Selenko, P. *J. Am. Chem. Soc.* **2010**, *132*, 14704–14705.
- (10) Dose, A.; Liokatis, S.; Theillet, F. X.; Selenko, P.; Schwarzer, D. *ACS Chem. Biol.* **2010**, *6*, 419–424.
- (11) Ashfield, J. T.; Meyers, T.; Lowne, D.; Varley, P. G.; Arnold, J. R.; Tan, P.; Yang, J. C.; Czaplowski, L. G.; Dudgeon, T.; Fisher, J. *Protein Sci.* **2000**, *9*, 2047–2053.
- (12) Macnaughtan, M. A.; Kane, A. M.; Prestegard, J. H. *J. Am. Chem. Soc.* **2005**, *127*, 17626–17627.
- (13) Abraham, S. J.; Kobayashi, T.; Solaro, R. J.; Gaponenko, V. *J. Biomol. NMR* **2009**, *43*, 239–246.
- (14) Couture, J. F.; Collazo, E.; Hauk, G.; Trievel, R. C. *Nat. Struct. Mol. Biol.* **2006**, *13*, 140–146.
- (15) Schanda, P.; Kupce, E.; Brutscher, B. *J. Biomol. NMR* **2005**, *33*, 199–211.
- (16) Del Rizzo, P. A.; Couture, J. F.; Dirk, L. M.; Strunk, B. S.; Roiko, M. S.; Brunzelle, J. S.; Houtz, R. L.; Trievel, R. C. *J. Biol. Chem.* **2010**, *285*, 31849–31858.
- (17) Couture, J. F.; Dirk, L. M.; Brunzelle, J. S.; Houtz, R. L.; Trievel, R. C. *Proc. Natl. Acad. Sci. U.S.A.* **2008**, *105*, 20659–20664.
- (18) Dhayalan, A.; Kudithipudi, S.; Rathert, P.; Jeltsch, A. *Chem. Biol.* **2011**, *18*, 111–120.

- (19) Esteve, P. O.; Patnaik, D.; Chin, H. G.; Benner, J.; Teitell, M. A.; Pradhan, S. *Nucleic Acids Res.* **2005**, *33*, 3211–3223.
- (20) Wu, H.; Min, J.; Lunin, V. V.; Antoshenko, T.; Dombrowski, L.; Zeng, H.; Allali-Hassani, A.; Campagna-Slater, V.; Vedadi, M.; Arrowsmith, C. H.; Plotnikov, A. N.; Schapira, M. *PLoS One* **2010**, *5*, e8570.
- (21) Wu, H.; Chen, X.; Xiong, J.; Li, Y.; Li, H.; Ding, X.; Liu, S.; Chen, S.; Gao, S.; Zhu, B. *Cell Res.* **2011**, *21*, 365–367.
- (22) Kouzarides, T. *Cell* **2007**, *128*, 693–705.
- (23) Saganuma, T.; Workman, J. L. *Annu. Rev. Biochem.* **2011**, *80*, 473–499.
- (24) Huang, J.; Dorsey, J.; Chuikov, S.; Perez-Burgos, L.; Zhang, X.; Jenuwein, T.; Reinberg, D.; Berger, S. L. *J. Biol. Chem.* **2010**, *285*, 9636–9641.
- (25) Chang, Y.; Zhang, X.; Horton, J. R.; Upadhyay, A. K.; Spannhoff, A.; Liu, J.; Snyder, J. P.; Bedford, M. T.; Cheng, X. *Nat. Struct. Mol. Biol.* **2009**, *16*, 312–317.
- (26) Haberland, M.; Montgomery, R. L.; Olson, E. N. *Nat. Rev. Genet.* **2009**, *10*, 32–42.
- (27) Kelly, T. K.; De Carvalho, D. D.; Jones, P. A. *Nat. Biotechnol.* **2010**, *28*, 1069–1078.
- (28) Spannhoff, A.; Hauser, A. T.; Heinke, R.; Sippl, W.; Jung, M. *ChemMedChem* **2009**, *4*, 1568–1582.
- (29) Copeland, R. A.; Solomon, M. E.; Richon, V. M. *Nat. Rev. Drug Discov.* **2009**, *8*, 724–732.